Antiprotozoal Steroidal Saponins from the Marine Sponge *Pandaros acanthifolium*

Erik L. Regalado,*[,†] Deniz Tasdemir,[‡] Marcel Kaiser,[§] Nadja Cachet,[⊥] Philippe Amade,[⊥] and Olivier P. Thomas*[,⊥]

Department of Chemistry, Center of Marine Bioproducts (CEBIMAR), Loma y 37 Alturas del Vedado, C.P. 10400 Havana, Cuba, Centre for Pharmacognosy and Phytotherapy, Department of Pharmaceutical and Biological Chemistry, School of Pharmacy, University of London, 29−39 Brunswick Square, London WC1N 1AX, United Kingdom, Department of Medical Parasitology and Infection Biology, Swiss Tropical Institute, 4002, Basel, Switzerland, and Laboratoire de Chimie des Molécules Bioactives et des Arômes, UMR 6001 CNRS, Institut de Chimie de Nice, Faculté des Sciences, University of Nice−Sophia Antipolis, Parc Valrose, 06108 Nice Cedex 2, France

Received May 24, 2010

The chemical composition of the Caribbean sponge *Pandaros acanthifolium* was reinvestigated and led to the isolation of 12 new steroidal glycosides, namely, pandarosides E−J (**1**−**6**) and their methyl esters (**7**−**12**). Their structures were determined on the basis of extensive spectroscopic analyses, including two-dimensional NMR and HRESIMS data. Like the previously isolated pandarosides A−D (**13**−**16**), the new compounds **1**−**12** share an unusual oxidized D-ring and a *cis* C/D ring junction. The absolute configurations of the aglycones were assigned by interpretation of CD spectra, whereas the absolute configurations of the monosaccharide units were determined by chiral GC analyses of the acid methanolysates. The majority of the metabolites showed *in vitro* activity against three or four parasitic protozoa. Particularly active were the compounds **3** (pandaroside G) and its methyl ester (**9**), which potently inhibited the growth of *Trypanosoma brucei rhodesiense* (IC_{50} values 0.78 and 0.038 μM, respectively) and *Leishmania donovani* (IC_{50}'s 1.3 and 0.051 μM, respectively).

Tropical diseases (TDs) are a group of chronic infections affecting about 1 billion people worldwide, mainly in Africa, South America, and Southeast Asia. Besides their massive negative impact on global health, TDs such as malaria, African trypanosomiasis (sleeping sickness), American trypanosomiasis (Chagas disease), and visceral leishmaniasis (kala azar) result in billions of dollars of lost productivity, an ongoing cycle of poverty, and social isolation.[1] Medicinal plants have provided excellent drug and drug templates for the treatment and control of parasitic diseases, especially malaria. During the last four decades marine invertebrates have been shown to produce highly active natural products with complex structural features. Despite their short history, marine natural products have found applications in therapeutic fields, particularly in cancer;[2,3] however their potential in antiprotozoal drug discovery has remained largely unexplored.

During our first investigation of the little-studied Caribbean marine sponge *Pandaros acanthifolium* (Poecilosclerida, Microcionidae), collected at the Canyon rock off the Martinique coast, steroidal saponins named pandarosides A−D (**13**−**16**), as well as their methyl esters (**17**−**19**), were identified as the major constituents of the sponge extract.[4] Before this, saponins had mostly been isolated from marine sponge of the genera *Asteropus* and *Erylus*.[5] This result was unexpected, as the order Poecilosclerida is best known to produce a large diversity of complex bioactive guanidine alkaloids.[6] The polyether acanthifolicin has been the only secondary metabolite reported from the *Pandaros* genus to date.[7] Acanthifolicin is an episulfur derivative of okadaic acid, a toxin identified as a major cause of diarrhetic shellfish poisoning. Because polyether toxins of this family were isolated from dinoflagellates, a microbial origin was also assumed for acanthifolicin.[8] We decided to reinvestigate the chemical composition of the extract in the search for bioactive constituents. We were not able to isolate the known acanthifolicin, and we report herein the isolation of six additional steroidal glycosides named pandarosides E−J (**1**−**6**) and their methyl esters (**7**−**12**) as constituents of the sponge *P. acanthifolium*. Their structures were elucidated by spectroscopic studies including 1D- and 2D-NMR experiments (COSY, HSQC, HMBC, and NOESY), as well as HRESIMS analyses. All of these metabolites, **1**−**12**, share a rare 2-hydroxycyclopent-2-enone D-ring with a β-configuration at C-14. Differences with the previously isolated pandarosides A−D reside in the B- and C-rings, in the alkyl side chain of the aglycone moiety, and in the sugar residues, where for the first time in this family xylose and rhamnose were identified. Only a few saponins have been found to exhibit antiprotozoal bioactivity;[9] however we decided to evaluate the potential of this new family of compounds. To this end, *in vitro* inhibitory activity of the new metabolites **1**−**12** and the previously isolated pandarosides **13**, **15**, and **16** and their methyl esters **17**, **18**, and **19** was evaluated against a small panel of parasitic protozoa, i.e., *Trypanosoma brucei rhodesiense* (bloodstream forms), *Trypanosoma cruzi* (intracellular amastigotes in L6 rat skeletal myoblasts), *Leishmania donovani* (axenic amastigotes), and *Plasmodium falciparum* (blood stage forms of K1 strain resistant to chloroquine and pyrimethamine). The compounds were also tested against recombinant *P. falciparum* fatty acid biosynthesis enzymes (*Pf*FabG, *Pf*FabI, *Pf*FabZ) in order to assess their potential in malaria prophylaxis.[10,11] The selectivity of the compounds toward L6 cells (a primary cell line derived from rat skeletal myoblasts) was also assessed.

Results and Discussion

The CH_2Cl_2/MeOH (1:1) extract of the Caribbean marine sponge *P. acanthifolium* was fractionated by RP-C_{18} flash chromatography, and a complex polar fraction was further purified by successive semipreparative RP-C_{18} HPLC and analytical C_6-phenyl HPLC to yield 12 new compounds, **1**−**6** together with their methyl esters **7**−**12**. Compound **1** had a molecular formula of $C_{39}H_{56}O_{14}$, as established by the HRESIMS analysis. The bands at 3496, 1692, and 1640 cm^{-1} in the IR spectrum suggested the presence of hydroxy and carbonyl functions. The NMR data were closely related to the previously isolated pandarosides A−D (**13**−**16**) (Tables 1 and 2).[5]

The 2-hydroxycyclopent-2-enone D-ring of the previously described pandarosides was present in **1** due to the signals at δ_C 58.8 (C-14), 201.0 (C-15), 151.5 (C-16), and 154.5 (C-17) in the ^{13}C NMR spectrum.[4] An additional tetrasubstituted unsaturation was evidenced by the new signals at δ_C 125.9 (C-8) and 142.4 (C-9).

* To whom correspondence should be addressed. E-mail: olivier.thomas@unice.fr. Phone: +33-4-92076134. Fax: +33-4-92076599.
† CEBIMAR Cuba.
‡ University of London.
§ Swiss Tropical Institute.
⊥ University of Nice−Sophia Antipolis.

10.1021/np100348x © 2010 American Chemical Society and American Society of Pharmacognosy
Published on Web 07/08/2010

Chart 1

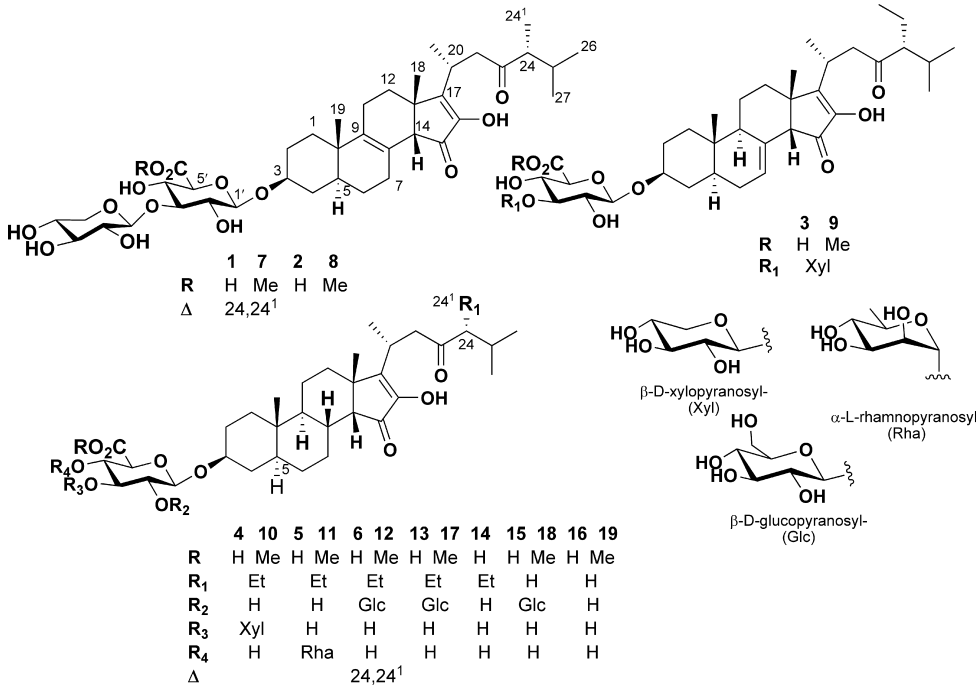

Table 1. ^{1}H NMR Data (500 MHz, CD_3OD) for Pandarosides **1**−**6** (δ in ppm, multiplicity (J in Hz))

no.	1	2	3	4	5	6
1β	1.72, m	1.73, m	1.79, m	1.68, m	1.64, m	1.68, m
1α	1.02, m	0.90, m	0.95, m	0.86, m	0.86, m	0.86, m
2α	1.90, m	1.90, m	1.85, m	1.85, m	1.85, m	1.86, m
2β	1.55, m	1.56, m	1.61, m	1.50, m	1.50, m	1.50, m
3	3.74, tt (10.5, 5.0)	3.67, m	3.49, m	3.64, tt (10.5, 5.0)	3.64, m	3.64, m
4α	1.78, m	1.78, m	2.42, m	1.70, m	1.72, m	1.72, m
4β	1.31, m	1.33, m	2.20, m	1.28, m	1.28, m	1.28, m
5	1.26, m	1.26, m	1.23, m	1.04, m	1.04, m	1.04, m
6α	1.58, m	1.58, m	2.99, m	1.35, m	1.35, m	1.35, m
6β	1.42, m	1.42, m	1.95, m	1.30, m	1.30, m	1.30, m
7α	2.67, m	2.67, m	5.42, dd (5.0, 2.0)	2.17, m	2.16, m	2.17, m
7β	1.89, m	1.90, m1.66, m	1.66, m	1.65, m		
8				1.94, m	1.94, m	1.94, m
9			2.02, dd (8.5, 5.5)	0.88, m	0.87, m	0.88, m
11β	2.00, m	2.00, m	1.43, m	1.39, m	1.38, m	1.39, m
11α	1.56, m	1.56, m	1.14, m	1.17, m	1.17, m	1.16, m
12β	1.92, m	1.93, m	1.59, m	1.55, m	1.55, m	1.55, m
12α	1.16, m	1.16, m	1.42, m	1.47, m	1.46, m	1.47, m
14	2.34, s	2.34, s	1.90, br s	1.84, d (4.5)	1.83, d (4.5)	1.85, d (4.5)
18	1.14, s	1.17, s	1.21, s	1.17, s	1.16, s	1.20, s
19	0.94, s	0.95, s	1.04, s	0.81, s	0.81, s	0.81, s
20	2.91, m	2.90, m	2.90, m	2.88, m	2.88, m	2.94, m
21	1.21, d (6.5)	1.18, d (7.0)	1.15, d (6.5)	1.15, d (7.0)	1.15, d (7.0)	1.19, d (6.5)
22a	3.19, dd (16.5, 8.5)	3.05, dd (18.0, 9.0)	2.97, dd (17.5, 9.0)	2.96, dd (17.5, 8.5)	2.97, dd (18.0, 8.5)	3.06, dd (16.5, 9.0)
22b	3.02, dd (16.5, 5.5)	2.79, dd (18.0, 4.5)	2.81, dd (17.5, 4.5)	2.79, dd (17.5, 4.5)	2.80, dd (18.0, 4.5)	2.94, dd (16.0, 4.5)
24		2.34, m	2.23, ddd (10.5, 7.5, 4.0)	2.23, ddd (10.0, 7.5, 4.0)	2.23, ddd (10.0, 7.5, 4.0)	
24^{1}a	6.12, s	1.01, d (7.0)	1.58, m	1.57, m	1.57, m	5.57, q (7.0)
24^{1}b	5.80, br s	1.51, m	1.52, m			
	1.53, m					
24^2			0.76, t (7.5)	0.76, t (7.5)	0.76, t (7.5)	1.67, d (7.0)
25	2.88, m	1.90, m	1.88, m	1.88, m	1.88, m	2.59, m
26/27	1.02, d (7.0)	0.88, d (6.5)	0.89, d (6.5)	0.89, d (6.5)	0.89, d (6.5)	1.02, d (6.5)
	1.04, d (7.0)	0.85, d (7.0)	0.90, d (6.5)	0.90, d (6.5)	0.90, d (6.5)	1.03, d (6.5)
1′	4.46, d (8.0)	4.50, d (8.0)	4.45, d (7.5)	4.48, d (8.0)	4.53, d (7.5)	4.57, d (7.5)
2′	3.37, t (8.0)	3.37, d (8.0)	3.37, t (8.0)	3.37, t (8.0)	3.38, t (9.5)	3.44, dd (9.0, 8.0)
3′	3.57, t (8.5)	3.56, m	3.56, t (8.5)	3.55, t (8.5)	3.51, m	3.60, t (9.0)
4′	3.55, t (8.5)	3.57, m	3.57, t (9.0)	3.56, t (8.5)	3.49, m	3.59, t (9.0)
5′	3.76, d (8.5)	3.77, d (8.5)	3.77, d (7.0)	3.81, d (9.5)	3.77, d (8.5)	3.78, d (8.0)
1″	4.55, d (7.5)	4.53, d (7.5)	4.55, d (7.5)	4.52, d (7.5)	5.17, d (1.5)	4.57, d (8.0)
2″	3.27, t (9.0)	3.27, t (8.5)	3.26, t (8.0)	3.27, t (9.0)	3.90, dd (3.0, 1.5)	3.24, t (8.0)
3″	3.33, t (9.0)	3.33, t (8.5)	3.33, t (9.0)	3.34, t (9.0)	3.64, dd (9.5, 3.5)	3.37, t (8.5)
4″	3.51, m	3.50, m	3.50, m	3.51, m	3.38, t (9.5)	3.33, m
5″a	3.91, dd (11.5, 5.0)	3.91, dd (11.5, 5.5)	3.90, dd (11.5, 5.0)	3.90, dd (11.5, 5.0)	4.11, tt (9.5, 6.5)	3.27, ddd (12.0, 5.0, 2.5)
5″b	3.22, dd (11.5, 9.0)	3.23, dd (11.5, 9.0)	3.23, dd (11.5, 9.0)	3.23, dd (11.5, 9.0)		
6″a					1.22, d (6.5)	3.84, dd (11.5, 2.5)
6″b						3.71, dd (11.5, 5.0)

Table 2. ^{13}C NMR Data (125 MHz, CD_3OD) for Pandarosides **1**−**6** (δ in ppm)

no.	1	2	3	4	5	6
1	34.9	34.9	37.8	37.4	37.5	37.5
2	29.9	30.0	30.2	30.0	30.0	30.0
3	78.7	79.5	79.7	79.9	79.0	79.8
4	34.9	35.0	39.3	35.3	35.2	35.4
5	42.4	42.4	43.7	45.6	45.6	45.7
6	26.6	26.6	30.2	30.3	30.3	30.2
7	32.1	32.1	123.3	31.3	31.4	31.3
8	125.9	126.0	141.4	35.1	35.0	35.1
9	142.4	142.3	31.1	45.8	45.9	45.9
10	38.2	38.2	40.0	38.3	38.3	38.3
11	22.8	22.8	19.1	19.9	20.0	20.0
12	34.6	34.7	31.9	32.6	32.6	32.2
13	43.6	43.7	43.9	43.7	43.7	43.7
14	58.8	58.9	54.3	56.1	56.1	56.1
15	201.0	201.4	205.7	206.0	206.0	206.5
16	151.5	151.3	151.6	151.4	151.5	151.5
17	154.5	155.0	153.5	154.9	154.8	155.0
18	28.6	28.5	25.6	25.8	25.9	25.9
19	17.0	17.0	18.0	11.1	11.2	11.2
20	29.1	27.4	27.3	27.3	27.3	27.7
21	18.6	18.5	17.9	17.9	18.0	18.0
22	43.6	47.3	49.0	49.0	49.0	48.3
23	203.2	215.9	215.8	215.8	215.8	209.9
24	157.0	54.4	61.9	61.9	61.9	150.6
24^1	123.0	13.0	22.3	22.3	22.3	124.1
24^2			12.3	12.3	12.3	15.0
25	29.0	31.2	30.8	30.8	30.8	32.2
26/27	22.4	19.2	20.0	20.0	20.0	22.2
	22.4	21.6	21.5	21.5	21.5	22.3
1′	101.7	102.3	102.0	102.4	100.4	101.4
2′	74.4	74.3	74.4	74.2	79.0	82.9
3′	86.2	86.5	86.0	86.7	73.4	73.3
4′	72.2	71.8	71.4	71.7	78.6	77.3
5′	76.8	76.4	76.7	76.4	76.7	76.2
6′	171.0	171.0	171.0	170.8	171.0	172.4
1″	105.5	105.8	106.0	105.9	102.3	105.2
2″	75.0	75.2	75.1	75.3	72.2	76.0
3″	77.6	77.6	77.6	77.6	72.4	77.7
4	71.0	71.0	71.0	71.0	73.9	71.4
5″	67.1	67.1	67.1	67.1	69.7	78.3
6″					18.0	62.7

The location of this unsaturation was deduced from the key H-14/C-8/C-9 and H_3-19/C-9 HMBC correlations (Figure 1). A *gem*-disubstituted C═C double bond was further evidenced by the signals at δ_H 5.80 (br s, 1H, H-24^1b) and 6.12 (s, 1H, H-24^1a) in the ^1H NMR spectrum of **1**. Its location at the C-24 position of the aglycone side chain was deduced from the key H-24^1a and H-24^1b/C-24, H_3-26/C-24, and H_3-27/C-24 HMBC correlations. Consequently, the aglycone skeleton of **1** belongs to the ergostane family of steroids, which is the first occurrence of this skeleton for a pandaroside.

Additionally, two sugar residues were evidenced in the HSQC spectrum of **1** by the characteristic signals of two anomeric protons at δ_H 4.46 (d, J = 8.0 Hz, 1H, H-1′), 4.55 (d, J = 7.5 Hz, 1H, H-1″) and δ_C 101.7 (C-1′), 105.5 (C-1″). The first sugar residue was identified as a glucuronic acid linked at C-3 to the aglycone

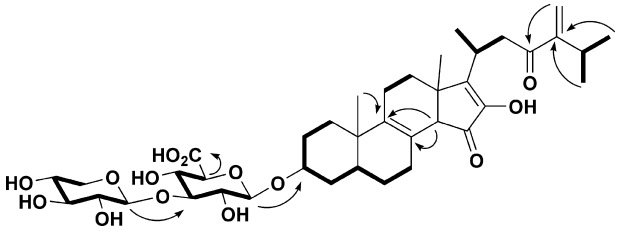

Figure 1. Key HMBC (H→C) and H−H COSY (−) correlations for **1**.

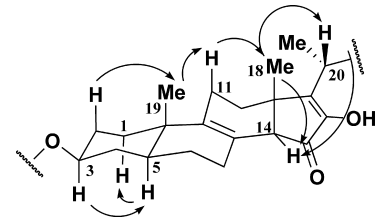

Figure 2. Key NOESY correlations for **1**.

core because of (a) the presence of a ^{13}C NMR signal at δ_C 171.0 (C-6′); (b) the values of the coupling constants of H-1′ (d, J = 8.0 Hz), H-2′ (t, J = 8.0 Hz), H-3′ (t, J = 8.5 Hz), H-4′ (t, J = 8.5 Hz), and H-5′ (d, J = 8.5 Hz); and (c) the key H-5′/C-6′ and H-1′/C-3 HMBC correlations. The second sugar residue was linked to the glucuronic acid at C-3′ because of the H-1″/C-3′ HMBC correlation. The deshielded AB system at δ_H 3.22 (dd, J = 11.5, 9.0 Hz, 1H, H-5″b) and 3.91 (dd, J = 11.5, 5.0 Hz, 1H, H-5″a) was characteristic of a cyclic pentose, which was further identified as a xylose by the coupling constant values of H-1″ (d, J = 7.5 Hz), H-2″ (t, J = 8.0 Hz), and H-3″ (t, J = 9.0 Hz).[12] The large coupling constant values for the doublets assigned to H-1′ and H-1″ (J = 8.0 and 7.5 Hz) implied that both sugars were connected through β-glycosidic linkages.

The relative configuration of the aglycone skeleton was found to be the same as for pandarosides A−D on the basis of NOE correlations and $^1H-^1H$ coupling constants analysis (Figure 2).[4] The positive Cotton effect at 262 nm ($\Delta\varepsilon$ = +7.0) in the CD spectrum of **1** was assigned to the $\pi\rightarrow\pi^*$ transition of the cyclopentenone ring because the enone of the side chain was located farther from a stereogenic center. Because a similar positive Cotton effect was observed for pandarosides A−D (**13**−**16**), we assumed the same absolute configuration for the aglycone part of **1**. This result was previously obtained by comparison between experimental and TDDFT-calculated CD spectra.[4] The absolute configuration of the sugar units was obtained by chiral GC analysis following acid methanolysis and acetylation of the sugar residues.[13]

The HRESIMS spectrum revealed a molecular formula of $C_{39}H_{58}O_{14}$ for compound **2**, which showed the presence of two additional protons in comparison to pandaroside E (**1**). The ^1H and ^{13}C NMR data were similar to those of **1**, which indicated the occurrence of a similar steroidal skeleton and sugar residues. Differences were located on the aglycone side chain, where the lack of signals at δ_H 6.12 (H-24^1a) and 5.80 (H-24^1b) and the presence of a doublet at δ_H 1.01 (d, J = 7.0 Hz, H_3-24^1) suggested that the C-24/C-24^1 bond was saturated in compound **2**. In the ^{13}C NMR spectrum of **2** the signals at δ_C 123.0 (C-24^1) and 157.0 (C-24) were replaced by new signals at δ_C 13.0 (C-24^1) and 54.4 (C-24), confirming this assumption. The 2-hydroxycyclopent-2-enone and the ketone gave rise to three Cotton effects of alternative signs at λ 330 ($\Delta\varepsilon$ = +5.6), 287 (−0.4), and 260 (+0.2) nm in the CD spectrum of **2**. The negative Cotton effect at 287 nm was assigned to the n→π^* transition of the side chain ketone, and the two others were assigned to electronic transitions of the enone. Because the same signs were observed for pandaroside A (**13**),[4] we assumed the same absolute configuration for the steroid skeleton but also for the side chain at C-24, which was previously deduced from comparison between experimental and calculated CD data.

Compound **3** had a molecular formula of $C_{40}H_{60}O_{14}$, which was determined from the HRESIMS spectrum. Comparing with the spectroscopic data of **2**, the additional methylene unit was located on the side chain of the aglycone core. Indeed the methyl signal of **2** at δ_H 1.01 (d, J = 7.0 Hz, H_3-24^1) was replaced by the signals of an ethyl group at δ_H 1.58 and 1.53 (m, H_2-24^1) and 0.76 (t, J = 7.0 Hz, H_3-24^2) in **3**. NMR data also indicated changes in the structure of the steroid skeleton (Table 1). The unsaturation previously located at C-8/C-9 for **1** and **2** was placed at C-7/C-8 in **3**, as deduced

from the presence of a new deshielded signal at δ_H 5.42 (dd, J = 5.0, 2.0 Hz, H-7) correlated in the COSY spectrum with the H_2-6 signals. The H-9 proton was placed on the α-face of the steroid skeleton on the basis of a NOE observed between H-9 and H-5. The sugar residues and the relative and absolute configurations were found to be the same as for **2** due to similar NMR and CD spectra.

The molecular formula of **4** was determined to be $C_{40}H_{62}O_{14}$ by HRESIMS, which represented the loss of an unsaturation compared to **3**. Both compounds exhibited very similar NMR spectra and were proven to share the same side chain and sugar residues. The structural difference was revealed by the absence of the NMR signals assigned for the C-7/C-8 unsaturation. H-8 was further placed on the β-face of the steroid skeleton on the basis of a NOE between H-8 and H_3-18.

The molecular formula of **5** was assigned as $C_{41}H_{64}O_{14}$ by HRESIMS. Comparison of the NMR spectra of **4** and **5** indicated that both aglycones were identical. However, significant changes were observed in the NMR spectra of one sugar residue. The glucuronic acid was still present at C-3, and the second residue was linked at C-4′ of this glucuronic acid, as indicated by a H-1″/C-4′ HMBC correlation. A new methyl signal at δ_H 1.22 (d, J = 6.5 Hz, H_3-6″) suggested the presence of a deoxy sugar. The identification of this deoxy sugar was performed by interpretation of the coupling constants of the corresponding ^{1}H NMR signals. Indeed, the H-1″ anomeric proton exhibited a signal at 5.17 (d, J = 1.5 Hz), which was consistent with an equatorial/equatorial relative configuration for H-1″ and H-2″. The conclusion was then made of an α-configuration for the linkage between both sugar residues, and interpretation of the remaining coupling constants led us to propose a rhamnose for the second sugar residue.[12] The same chiral GC analysis allowed us to propose the usual L absolute configuration for this sugar.[13]

Compound **6** exhibited the molecular formula $C_{41}H_{62}O_{15}$, as indicated by HRESIMS. Strong similarities between ^{1}H and ^{13}C NMR data of compounds **4**, **5**, and **6** allowed us to propose the same steroid backbone for the three compounds. The COSY correlated signals at δ_H 5.57 (q, J = 7.0 Hz, H-24^1) and 1.67 (d, J = 7.0 Hz, H_3-24^2) were reminiscent of the presence of an unsaturation on the side chain of **6**. Location of this unsaturation at C-24 was realized on the basis of the C-24/H-25/H-24^1 HMBC correlations. The configuration of this C=C double bond was assigned as *Z* due to a NOE between H-24^1 and H_3-26. Looking now at the sugar residues, the characteristic glucuronic acid was present at C-3 and a glucose residue was placed at C-2′ because of a H-2″/C-1′ HMBC correlation just as for pandarosides A (**13**) and C (**15**).[4] Compound **6** was therefore identified as the C-24/C-24^1 didehydro derivative of pandaroside A (**13**). The chiral GC analysis demonstrated a D configuration for this glucose residue.

The molecular formula of **7** ($C_{40}H_{58}O_{14}$), calculated from the HRESIMS spectrum, indicated the presence of an additional methylene unit in comparison with **1**. The ^{1}H and ^{13}C NMR data were very similar to those of **1** except for the new signals at δ_H 3.76 (s, $\underline{H}_3$-CO) and δ_C 53.0 (O-$\underline{C}H_3$), which suggested the presence of a methoxy group. The H_3-CO/C-6′ HMBC correlation allowed the identification of this compound as the methyl ester of pandaroside E (**1**). For all pandarosides (**2**−**6**), their methyl esters were isolated and characterized in the same manner as for the methyl ester of pandaroside E (**7**). These methyl esters may be artifacts formed from **1**−**6** during the MeOH extraction steps.Very similar CD spectra were obtained for all new metabolites (**2**−**12**), which suggested the same absolute configuration for their aglycone.

Table 3 shows the *in vitro* antiprotozoal activity and cytotoxicity of the new compounds, as well as the previously isolated pandarosides and their methyl esters. Note that compound **14** was not tested due to the small amount isolated. Except for pandaroside H (**4**), all new compounds inhibited the growth of all four parasitic protozoa. Against *T. b. rhodesiense* and *T. cruzi*, pandaroside G methyl ester (**9**) was the most active, with IC_{50} values of 0.038 and 0.77 μM, respectively, followed by the parent compounds pandaroside G (**3**) and pandaroside F (**2**) (Table 3). Notably, **9** was more active against *T. cruzi* cultures than the standard compound benznidazole (IC_{50} 2.64 μM). A similar trend was observed against the remaining parasites, *L. donovani* and *P. falciparum*. The potency of compound **9** against *L. donovani* (IC_{50} value 0.051 μM) was 10 times higher than that of the control drug, miltefosine (IC_{50} 0.505 μM). Compound **9** exhibited a sub-micromolar level antimalarial activity against the multidrug-resistant strain of *P. falciparum* (IC_{50} 0.38 μM). Compounds **3** and **2** were again the second and third best leishmanicidal and plasmocidal metabolites, with IC_{50} values in the low micromolar range. When tested for cytotoxicity toward L6 cells, a primary cell line derived from mammalian (rat) skeletal myoblasts, compounds **9**, **3**, and **2** appeared to have the highest toxic potential. This indicates that these compounds have general toxicity, with some selectivity against *T. b. rhodesiense* and *L. donovani*. The known pandarosides and their methyl esters had generally weak antiprotozoal potencies. The only exception was pandaroside D methyl ester (**19**), which inhibited the growth of *P. falciparum* with an IC_{50} value of 5.1 μM. Accordingly, the known pandarosides exhibited low or no toxicity against L6 cells. The least active compound was pandaroside C (**15**), which was almost inactive in all parasite or toxicity assays. The compounds were also tested against recombinant *P. falciparum* fatty acid biosynthesis enzymes (*Pf*FabG, *Pf*FabI, and *Pf*FabZ) in order to assess their potential in malaria prophylaxis. None of the compounds were active at 20 μg/mL concentration.

Table 3. *In Vitro* Antiprotozoal and Cytotoxic Activities of Sponge-Derived Compounds **1**−**19** (IC_{50} values in μM)

compound	*T. b. rhodesiense*	*T. cruzi*	*L. donovani*	*P. falciparum*	cytotoxicity
1	9.4	71.6	15.9	13.8	40.9
2	2.4	20.3	4.3	5.7	10.8
3	0.8	9.7	1.3	2.5	5.4
4	68.4	>120	46.7	22.8	>120
5	19.2	70.8	36.0	>25	>120
6	14.5	83.4	36.1	24.3	78.0
7 (1-Me)[f]	14.3	61.9	41.3	5.9	76.9
8 (2-Me)	54.4	25.1	26.8	9.9	42.1
9 (3-Me)	**0.038**	**0.77**	**0.051**	**0.39**	**0.22**
10 (4-Me)	19.9	36.1	16.5	10.2	43.3
11 (5-Me)	27.2	21.7	28.7	13.0	59.6
12 (6-Me)	15.6	70.5	20.7	12.4	75.2
13	9.1	52.2	19.7	17.6	48.9
14	n.t.[g]	n.t.	n.t.	n.t.	n.t.
15	66.4	>120	>120	>25	>120
16	15.3	80.8	31.0	13.5	96.6
17 (13-Me)	114	>120	66.3	>25	>120
18 (15-Me)	61.4	100	44.2	>25	>120
19 (16-Me)	40.4	21.6	13.7	5.1	106
standards	0.010[a]	2.64[b]	0.51[c]	0.2[d]	0.012[e]

[a] Standard compound melarsoprol. [b] Standard compound benznidazole. [c] Standard compound miltefosine. [d] Standard compound chloroquine. [e] Standard compound podophyllotoxin. [f] Me: methyl ester. [g] n.t. not tested.

It was noteworthy that, with a few exceptions, pandaroside methyl esters were generally much more active and toxic against parasitic and mammalian cells. The best example for this assumption is represented by the pair **3** and **9**. The situation was *vice versa* in the pairs of **2/8** and **13/17**, whereas pandaroside J (**6**) and its methyl ester (**12**) have exerted almost identical IC_{50} values in all assays. The methyl esters may act as prodrugs, allowing easier entry into the cells, where they could be hydrolyzed to the corresponding acids that have the cytotoxic activity. Some additional structure−activity relationships on the aglycone were drawn from these results. The presence of an additional exocyclic double bond at C-24, as exemplified by **1**, seems not to be favored, as compound **2**, which lacks $\Delta^{24,241}$ is more potent than **1**. Importantly, the presence of an ethyl substitution at C-24 and the shift of the double bond from $\Delta^{8,9}$ to $\Delta^{7,8}$ (as in the case of **3**) appear to be essential for bioactivity,

but this also increases the cytotoxicity. The striking differences in the bioactivity of **3** and **4**, which differ from each other by the presence of $\Delta^{7,8}$ suggests that an unsaturation at this position is crucial for antiprotozoal potential and cytotoxicity. Compound **6**, which has an unsaturation at C-24 but lacks an additional double bond in ring B, does not show significant antiparasitic or cytotoxic potential. The low potency of **6** in comparison to **1**−**3** points out, one more time, the importance of an additional cyclic double bond in ring B. On the other hand, the exact impact of the position and the nature of additional sugar units remains unclear. It is likely that the attachment of a terminal xylose function at the C-3′ position of the inner glucose molecule is favored for the activity.

This study underlines and extends the large diversity of steroidal glycosides from the pandaroside family produced by the Caribbean marine sponge *P. acanthifolium*. For the first time in this family, unsaturations were present on the B and C cycles of the steroid skeleton, the diversity of sugar residues now includes xylose and rhamnose, rarely found in marine organisms, and finally exo unsaturations at C-24 were described for some pandarosides. Such oxygenated steroids with an enone on the side chain have already been isolated from Chinese soft corals,[14−16] but they all share an ergostane skeleton. Consequently, pandaroside J (**6**) and its methyl ester (**12**) are the first examples of steroids with a keto conjugated ethylidene at C-24. Pandarosides are new steroid saponins of the cholestane, poriferastane, and now ergostane families sharing a 2-hydroxycyclopent-2-enone, a *cis* C/D ring junction, and a C-23 ketone function. In the marine environment some of these features were also present in compounds produced by marine sponges,[17,18] but to our knowledge, pandarosides are the first example of steroids featuring a 2-hydroxycyclopent-2-enone D-ring with a 14β-configuration isolated from a marine source. These very rare features have appeared in only two steroids isolated from an Egyptian plant.[19]

The current study shows that the minor pandarosides, particularly pandaroside G methyl ester (**11**), pandaroside G (**3**), and pandaroside F (**2**), have promising antiprotozoal potential, but also possess cytotoxicity. Pregnane glycosides isolated from octocorals have been found to be moderately active against *P. falciparum*.[20,21] To our knowledge, this is the first study assessing the antiprotozoal activity of marine cholestane, poriferastane, and ergostane glycosides.

Experimental Section

General Experimental Procedures. Optical rotations were measured on a polarimeter equipped with a 10 cm microcell. UV measurements were performed on a UV−visible spectrophotometer. CD spectra were measured using a spectropolarimeter. IR spectra were obtained with a FT-IR spectrophotometer. NMR experiments were performed on a 500 MHz spectrometer. Chemical shifts (δ in ppm) are referenced to the carbon (δ_C 49.0) and residual proton (δ_H 3.31) signals of CD_3OD, the solvent with multiplicity (s singlet, d doublet, t triplet, m multiplet). Electrospray ionization (ESI) mass spectra were obtained with a mass spectrometer in the positive or negative mode. High-resolution mass spectra (HRESIMS) were obtained from a mass spectrometer. Flash chromatography fractionation was performed on an instrument equipped with a UV detector. HPLC separation and purification were carried out on a system equipped with a photodiode array detector coupled with a ELSD and an autosampler. TLC was performed with Kieselgel 60 F_{254}, and spots were detected after spraying with 10% H_2SO_4 in EtOH reagent and heating.

Biological Material. The marine sponge *Pandaros acanthifolium* was collected off Martinique Island in the summer of 2003 by scuba diving at a depth of 19 m (Canyons de Babodie 14°45,982 N, 61°11,902 W). A voucher specimen (ORMA8362), identified by Dr. Jean Vacelet, has been deposited in the Centre d'Océanologie de Marseille (Endoume, France). The sponge was kept frozen from collection until the extraction process.

Extraction and Isolation. The second portion of the previously studied frozen sponge (536 g) was cut into pieces of about 1 cm^3 and extracted with 1:1 MeOH/CH_2Cl_2 at room temperature, yielding 20.0 g of extract after solvent evaporation. The crude extract was fractionated by RP-C_{18} flash chromatography (elution with a decreasing polarity gradient of H_2O/MeOH from 1:0 to 0:1, then MeOH/CH_2Cl_2 from 1:0 to 0:1). The 1:3 H_2O/MeOH (220 mg) fraction was then subjected to RP-C_{18} semipreparative HPLC (250 × 10 mm, 5 μm) with a gradient of H_2O/MeOH/TFA (flow 3.0 mL min^{-1} from 28:72:0.1 to 20:80:0.1) to obtain a complex chemical profile (see Supporting Information). The subsequent mixtures were finally purified by analytical HPLC (C_6-phenyl, 250 × 3 mm, 5 μm) with a gradient of H_2O/CH_3CN/formic acid (flow 0.5 mL min^{-1}, from 65:35:0.1 to 50:50:0.1) to afford pure compounds **1** (1.5 mg, 0.3 × 10^{-3}% w/w), **2** (1.0 mg, 0.3 × 10^{-3}% w/w), **3** (2.9 mg, 0.5 × 10^{-3}% w/w), **4** (1.8 mg, 0.3 × 10^{-3}% w/w), **5** (2.9 mg, 0.5 × 10^{-3}% w/w), **6** (1.3 mg, 0.2 × 10^{-3}% w/w), **7** (3.0 mg, 0.6 × 10^{-3}% w/w), **8** (2.8 mg, 0.5 × 10^{-3}% w/w), **9** (3.5 mg, 0.7 × 10^{-3}% w/w), **10** (2.1 mg, 0.4 × 10^{-3}% w/w), **11** (5.5 mg, 1.0 × 10^{-3}% w/w), and **12** (0.9 mg, 0.2 × 10^{-3}% w/w).

Pandaroside E (1): 16-hydroxy-3β-*O*-[β-D-xylopyranosyl-(1→3)-β-D-glucopyranosyloxyuronic acid]-5α,14β-ergosta-8,16,24(24^1)-triene-15,23-dione; white, amorphous solid; $[\alpha]^{20}_D$ +30.0 (*c* 0.10, MeOH); UV (MeOH) λ_{max} (log ε) 263 (3.98) nm; CD (MeOH, *c* 3.3 × 10^{-4} M) λ_{max} ($\Delta\varepsilon$) 262 (+7.6), 320 (−0.3) nm; IR (thin film) ν_{max} 3496, 1692, 1640, 1199, 1132 cm^{-1}; ^{1}H NMR see Table 1; ^{13}C NMR see Table 2; HRESIMS (+) *m*/*z* 771.3570 $[M + Na]^+$ (calcd for $C_{39}H_{56}NaO_{14}$, 771.3568, Δ 0.3 ppm).

Pandaroside F (2): 16-hydroxy-3β-*O*-[β-D-xylopyranosyl-(1→3)-β-D-glucopyranosyloxyuronic acid]-5α,14β-ergost-8,16-diene-15,23-dione; white, amorphous solid; $[\alpha]^{20}_D$ +52.7 (*c* 0.16, MeOH); UV (MeOH) λ_{max} (log ε) 264 (3.76) nm; CD (MeOH, *c* 5.0 × 10^{-4} M) λ_{max} ($\Delta\varepsilon$) 260 (+5.6), 287 (−0.4), 330 (+0.2) nm; IR (thin film) ν_{max} 3412, 1697, 1677, 1196 cm^{-1}; ^{1}H NMR see Table 1; ^{13}C NMR see Table 2; HRESIMS (+) *m*/*z* 773.3727 $[M + Na]^+$ (calcd for $C_{39}H_{58}NaO_{14}$, 773.3724, Δ 0.4 ppm).

Pandaroside G (3): 16-hydroxy-3β-*O*-[β-D-xylopyranosyl-(1→3)-β-D-glucopyranosyloxyuronic acid]-5α,14β-poriferasta-7,16-diene-15,23-dione; white, amorphous solid; $[\alpha]^{20}_D$ +16.8 (*c* 0.07, MeOH); UV (MeOH) λ_{max} (log ε) 264 (3.91) nm; CD (MeOH, *c* 3.3 × 10^{-4} M) λ_{max} ($\Delta\varepsilon$) 260 (+5.1), 290 (−0.9), 327 (+0.9) nm; IR (thin film) ν_{max} 3418, 1691, 1672, 1182 cm^{-1}; ^{1}H NMR see Table 1; ^{13}C NMR see Table 2; HRESIMS (+) *m*/*z* 787.3884 $[M + Na]^+$ (calcd for $C_{40}H_{60}NaO_{14}$, 787.3881, Δ 0.4 ppm).

Pandaroside H (4): 16-hydroxy-3β-*O*-[β-D-xylopyranosyl-(1→3)-β-D-glucopyranosyloxyuronic acid]-5α,14β-poriferast-16-ene-15,23-dione; white, amorphous solid; $[\alpha]^{20}_D$ +9.1 (*c* 0.08, MeOH); UV (MeOH): λ_{max} (log ε) 263 (3.92) nm; CD (MeOH, *c* 3.0 × 10^{-4} M) λ_{max} ($\Delta\varepsilon$) 262 (+5.1), 290 (−1.6), 327 (+1.1) nm; IR (thin film) ν_{max} 3421, 1684, 1670, 1198 cm^{-1}; ^{1}H NMR see Table 1; ^{13}C NMR see Table 2; HRESIMS (+) *m*/*z* 789.4041 $[M + Na]^+$ (calcd for $C_{40}H_{62}NaO_{14}$, 789.4037, Δ 0.5 ppm).

Pandaroside I (5): 16-hydroxy-3β-*O*-[α-rhamnopyranosyl-(1→4)-β-D-glucopyranosyloxyuronic acid]-5α,14β-poriferast-16-ene-15,23-dione; white, amorphous solid; $[\alpha]^{24}_D$ −13.0 (*c* 0.10, MeOH); UV (MeOH) λ_{max} (log ε) 264 (3.90) nm; CD (MeOH, *c* 3.2 × 10^{-4} M) λ_{max} ($\Delta\varepsilon$) 260 (+3.5), 287 (−1.4), 326 (+0.7) nm; IR (thin film) ν_{max} 3338, 1731, 1669, 1193 cm^{-1}; ^{1}H NMR see Table 1; ^{13}C NMR see Table 2; HRESIMS (+) *m*/*z* 803.4201 $[M + Na]^+$ (calcd for $C_{41}H_{64}NaO_{14}$, 803.4194, Δ 0.9 ppm).

Pandaroside J (6): 3β-*O*-[β-D-glucopyranosyl-(1→2)-β-D-glucopyranosyloxyuronic acid]-16-hydroxy-5α,14β-poriferasta-16,24(24^1)-diene-15,23-dione; white, amorphous solid; $[\alpha]^{20}_D$ +4.0 (*c* 0.10, MeOH); UV (MeOH) λ_{max} (log ε) 265 (4.00) nm; CD (MeOH, *c* 3.3 × 10^{-4} M) λ_{max} ($\Delta\varepsilon$) 262 (+3.7), 330 (+1.0) nm; IR (thin film) ν_{max} 3425, 1696, 1680, 1195 cm^{-1}; ^{1}H NMR see Table 1; ^{13}C NMR see Table 2; HRESIMS (+) *m*/*z* 817.3982 $[M + Na]^+$ (calcd for $C_{41}H_{62}NaO_{15}$, 817.3986, Δ −0.5 ppm).

Methyl Ester of Pandaroside E (7): white, amorphous solid; $[\alpha]^{20}_D$ +37.0 (*c* 0.10, MeOH); ^{1}H NMR (500 MHz, CD_3OD) for the uronic residue, δ 4.50 (d, *J* = 7.9 Hz, H-1′), 3.37 (t, *J* = 8.0 Hz, H-2′), 3.57 (t, *J* = 9.0 Hz, H-3′), 3.59 (t, *J* = 8.8 Hz, H-4′), 3.87 (d, *J* = 9.5, H-5′), 3.76 (s, CH_3O−); ^{13}C NMR (125 MHz, CD_3OD) for the uronic residue, 102.5 (C-1′), 74.2 (C-2′), 86.4 (C-3′), 71.6 (C-4′), 76.4 (C-5′), 171.0 (C-6′), 52.8 (CH_3O−); HRESIMS (+) *m*/*z* 785.3720 $[M + Na]^+$ (calcd for $C_{40}H_{58}NaO_{14}$, 785.3724, Δ −0.5 ppm).

Methyl Ester of Pandaroside F (8): white, amorphous solid; $[\alpha]^{20}_D$ +47.3 (*c* 0.10, MeOH); ^{1}H NMR (500 MHz, CD_3OD) for the uronic residue, δ 4.50 (d, *J* = 7.9 Hz, H-1′), 3.36 (t, *J* = 8.5 Hz, H-2′), 3.55 (t, *J* = 8.8 Hz, H-3′), 3.59 (t, *J* = 9.0 Hz, H-4′), 3.87 (d, *J* = 9.2,

H-5′), 3.76 (s, CH_3O−); ^{13}C NMR (125 MHz, CD_3OD) for the uronic residue, 102.5 (C-1′), 74.2 (C-2′), 86.4 (C-3′), 71.6 (C-4′), 76.4 (C-5′), 171.0 (C-6′), 52.9 (CH_3O−); HRESIMS (+) *m/z* 787.3882 $[M + Na]^+$ (calcd for $C_{40}H_{60}NaO_{14}$, 787.3881, Δ 0.1 ppm).

Methyl Ester of Pandaroside G (9): white, amorphous solid; $[\alpha]^{20}_D$ +30.0 (*c* 0.10, MeOH); ^1H NMR (500 MHz, CD_3OD) for the uronic residue, δ 4.50 (d, *J* = 7.9 Hz, H-1′), 3.37 (t, *J* = 8.0 Hz, H-2′), 3.57 (t, *J* = 9.0 Hz, H-3′), 3.59 (t, *J* = 8.8 Hz, H-4′), 3.89 (d, *J* = 9.0, H-5′), 3.76 (s, CH_3O−); ^{13}C NMR (125 MHz, CD_3OD) for the uronic residue, 102.7 (C-1′), 74.2 (C-2′), 86.3 (C-3′), 71.6 (C-4′), 76.4 (C-5′), 171.0 (C-6′), 52.9 (CH_3O−); HRESIMS (+) *m/z* 801.4040 $[M + Na]^+$ (calcd for $C_{41}H_{62}NaO_{14}$, 801.4037, Δ 0.4 ppm).

Methyl Ester of Pandaroside H (10): white, amorphous solid; $[\alpha]^{20}_D$ +7.4 (*c* 0.08, MeOH); ^1H NMR (500 MHz, CD_3OD) for the uronic residue, δ 4.49 (d, *J* = 7.9 Hz, H-1′), 3.36 (t, *J* = 8.0 Hz, H-2′), 3.57 (t, *J* = 8.8 Hz, H-3′), 3.59 (t, *J* = 8.9 Hz, H-4′), 3.87 (d, *J* = 9.4, H-5′), 3.76 (s, CH_3O−); ^{13}C NMR (125 MHz, CD_3OD) for the uronic residue, 102.5 (C-1′), 74.2 (C-2′), 86.4 (C-3′), 71.6 (C-4′), 76.4 (C-5′), 171.0 (C-6′), 52.8 (CH_3O−); HRESIMS (+) *m/z* 803.4186 $[M + Na]^+$ (calcd for $C_{41}H_{64}NaO_{14}$, 803.4194, Δ −1.0 ppm).

Methyl Ester of Pandaroside I (11): white, amorphous solid; $[\alpha]^{20}_D$ −11.7 (*c* 0.18, MeOH); ^1H NMR (500 MHz, CD_3OD) for the uronic residue, δ 4.55 (d, *J* = 7.6 Hz, H-1′), 3.37 (t, *J* = 8.0 Hz, H-2′), 3.49 (dd, *J* = 9.1 3.5, H-3′), 3.49 (d, *J* = 2.7 Hz, H-4′); 3.83 (d, *J* = 9.0 Hz, H-5′), 3.77 (s, CH_3O−); ^{13}C NMR (125 MHz, CD_3OD) for the uronic acid residue, 100.8 (C-1′), 78.8 (C-2′), 73.3 (C-3′), 78.6 (C-4′), 76.5 (C-5′), 171.2 (C-6′), 52.8 (CH_3O−); HRESIMS (+) *m/z* 817.4354 $[M + Na]^+$ (calcd for $C_{42}H_{66}NaO_{14}$, 817.4350, Δ 0.5 ppm).

Methyl Ester of Pandaroside J (12): white, amorphous solid; $[\alpha]^{20}_D$ +2.4 (*c* 0.08, MeOH); ^1H NMR (500 MHz, CD_3OD) for the uronic residue, δ 4.60 (d, *J* = 7.6 Hz, H-1′), 3.43 (t, *J* = 7.5 Hz, H-2′), 3.56 (m, H-3′ and H-4′), 3.83 (d, *J* = 9.5 Hz, H-5′), 3.76 (s, CH_3O−); ^{13}C NMR (125 MHz, CD_3OD) for the uronic residue, 102.0 (C-1′), 82.9 (C-2′), 73.1 (C-3′), 77.1 (C-4′), 76.6 (C-5′), 171.3 (C-6′), 53.0 (CH_3O−); HRESIMS (+) *m/z* 831.4141 $[M + Na]^+$ (calcd for $C_{42}H_{64}NaO_{15}$, 831.4143, Δ −0.2 ppm).

Methanolysis of Pandarosides. Compounds **1**, **3**, **5**, and **6** (0.30 mg each) were dissolved in a HCl (7 N, 1.0 mL)/MeOH solution and heated at 75 °C for 4 h. The reaction mixtures were neutralized with $NaHCO_3$, evaporated to dryness, and then partitioned between $CHCl_3$ and H_2O. The H_2O layer was dried under reduced pressure to afford mixtures of methyl glycosides.

Derivatization of the Hydrolysate for GC Analysis. The methanolysis products were dissolved in a mixture of dry CH_2Cl_2/pyridine (1:1), and an excess of acetic anhydride was added. The reaction was stirred at 25 °C for 8 h. The mixture was then dried and dissolved in EtOAc for GC analysis.

Chiral GC Analysis. GC analysis was carried out on a Chirasil-L-Val capillary column (25 m × 0.25 mm, i.d.), using a mass selective detector. A temperature gradient system was used for the oven, starting at 100 °C for 3 min and increasing up to 200 °C at a rate of 10 °C/min. Peaks of the hydrolysates of the pandarosides and sugar standards were detected at 15.3 min (D-glc), 13.2 min (D-xyl), 12.1 min (D-glcUA), and 11.5 min (L-rha). Because some retention times fluctuated, the identity of the enantiomers was confirmed by injection of a mixture of the sample and standards acetylated using the same protocol.

Antimalarial Activity against *P. falciparum*. *In vitro* parasite growth inhibition was assessed by a modified [^3H]-hypoxanthine incorporation assay using the chloroquine- and pyrimethamine-resistant K1 strain and the standard drug chloroquine. Briefly, compounds were dissolved in 100% DMSO, and 2-fold dilution series of the compounds prepared in assay medium (RPMI 1640 supplemented with 5% Albumax II, 0.2% w/v glucose, 0.03% L-glutamine) were added to each well of the microtiter plates. Parasite cultures (50 μL) were added to each well, reaching a final volume of 100 μL per well (final DMSO concentration ≤0.25%). Plates were incubated at 37 °C for 48 h, and 0.1 μCi ^3H-hypoxanthine (Perkin-Elmer) was added to each well. The plates were mixed and incubated for another 24 h. The experiment was terminated by placing the plates in a −80 °C freezer. Plates were thawed and harvested onto glass fiber filter mats using a 96-well cell harvester (Harvester 96, Tomtec). The incorporated radioactivity was counted using a liquid Betalux scintillation counter (Wallac). Data acquired by the Wallac BetaLux scintillation counter were exported into a Microsoft Excel spreadsheet, and the IC_{50} values of each compound were calculated.

Plasmodial FAS-II Enzyme Inhibition Assays. Expression and purification of the *Pf*Fab enzymes were performed as described.[22] All measurements were performed on a spectrophotometer in 1 mL of 20 mM HEPES, pH 7.4, and 150 mM NaCl. Compounds were dissolved in DMSO. For *Pf*FabI, 100 μM NADH (cofactor) was added to 1 μg of enzyme, and the reaction was started by addition of the substrate (crotonyl-CoA, 50 μM). The mixture was read spectrophotometrically for 1 min at 340 nm. For *Pf*FabG assays, NADPH (cofactor) and acetoacetyl-CoA (substrate) were used. *Pf*FabZ activity was measured at 263 nm for 5 min in the presence of 25 μM crotonoyl-CoA and 0.5 μg of enzyme. Reference compounds were triclosan (*Pf*FabI) and (−)-catechin gallate (*Pf*FabG, *Pf*FabZ). IC_{50} values were estimated from graphically plotted dose−response curves.

Trypanocidal Activity against *T. brucei rhodesiense*. The STIB 900 strain parasite and the standard drug melarsoprol were used for the assay. Minimum essential medium (50 μL) supplemented with 25 mM HEPES, 1 g/L additional glucose, 1% MEM nonessential amino acids (100×), 0.2 mM 2-mercaptoethanol, 1 mM Na-pyruvate, and 15% heat-inactivated horse serum was added to each well of a 96-well microtiter plate.[23,24] Serial drug dilutions of seven 3-fold dilution steps covering a range from 90 to 0.12 μg/mL were prepared. Then 10^4 bloodstream forms of *T. b. rhodesiense* STIB 900 in 50 μL were added to each well, and the plates were incubated at 37 °C under a 5% CO_2 atmosphere for 72 h. A 10 μL portion of a resazurin solution (12.5 mg of resazurin dissolved in 100 mL of double-distilled water) was then added to each well, and incubation continued for a further 2−4 h.[25] Then the plates were read in a microplate fluorometer using an excitation wavelength of 536 nm and an emission wavelength of 588 nm. Data were analyzed using a microplate reader software.

Trypanocidal Activity against *Trypanosoma cruzi*. Rat skeletal myoblasts (L6 cells) were seeded in 96-well microtiter plates at 2000 cells/well in 100 μL of RPMI 1640 medium with 10% FBS and 2 mM L-glutamine. After 24 h the medium was removed and replaced by 100 μL per well containing 5000 trypomastigote forms of *T. cruzi* Tulahuen strain C2C4 containing the β-galactosidase (Lac Z) gene.[26] After 48 h, the medium was removed from the wells and replaced by 100 μL of fresh medium with or without a serial drug dilution of seven 3-fold dilution steps covering a range from 90 to 0.12 μg/mL. After 96 h of incubation the plates were inspected under an inverted microscope to ensure growth of the controls and sterility. Then the substrate CPRG/Nonidet (50 μL) was added to all wells. A color reaction developed within 2−6 h and was read photometrically at 540 nm. Data were transferred into a specific program, which calculated IC_{50} values.

Leishmanicidal Activity against *Leishmania donovani*. Amastigotes of *L. donovani* strain MHOM/ET/67/L82 were grown in axenic culture at 37 °C in SM medium at pH 5.4 supplemented with 10% heat-inactivated fetal bovine serum under an atmosphere of 5% CO_2 in air. Then 100 μL of culture medium with 10^5 amastigotes from axenic culture with or without a serial drug dilution was seeded in 96-well microtiter plates. Serial drug dilutions covering a range from 90 to 0.12 μg/mL were prepared. After 72 h of incubation the plates were inspected under an inverted microscope to ensure growth of the controls and sterile conditions. A resazurin solution (10 μL) was then added to each well, and the plates were incubated for another 2 h.[27] Then the plates were read in a Spectramax Gemini XS microplate fluorometer using an excitation wavelength of 536 nm and an emission wavelength of 588 nm. Data were analyzed using a software. Decrease of fluorescence (= inhibition) was expressed as percentage of the fluorescence of control cultures and plotted against the drug concentrations. From the sigmoidal inhibition curves the IC_{50} values were calculated.

Cytotoxicity against L6 Cells. Assays were performed in 96-well microtiter plates, each well containing 100 μL of RPMI 1640 medium, supplemented with 1% L-glutamine (200 mM) and 10% fetal bovine serum, and 4 × 10^4 L6 cells. Serial drug dilutions of seven 3-fold dilution steps covering a range from 90 to 0.12 μg/mL were prepared. After 72 h of incubation the plates were inspected under an inverted microscope to ensure growth of the controls and sterile conditions. Alamar Blue (10 μL, 12.5 mg of resazurin dissolved in 100 mL of double-distilled water) was then added to each well, and the plates were incubated for another 2 h. Then the plates were read with a microplate fluorometer using an excitation wavelength of 536 nm and an emission wavelength of 588 nm. Data were analyzed using a microplate reader software. Podophyllotoxin was the standard drug used.

Acknowledgment. We are grateful to PharmaMar Madrid for financial support and for a grant (N.C.) of the Région Provence-Alpes-Côte d'Azur. We are also grateful to UNESCO and Boehringer Ingelheim Fonds for financial support provided by two fellowships (E.L.R.). We thank J. Vacelet (Centre d'Océanologie de Marseille) for careful taxonomical sponge identification, M. Gaysinski and the PFTC of Nice for assistance in recording the NMR spectroscopic experiments, J.-M. Guigonis for assistance in recording the HRMS experiments, and C. M. Jiménez and A. D. Rodríguez for assistance in GC analyses. We finally thank Mr le préfet de la Martinique and the DIREN for their help in the collection of Caribbean marine invertebrates.

Supporting Information Available: ^{1}H, ^{13}C, and 2D NMR spectra for compounds **1**−**6** and their methyl esters **7**−**12** and a CD spectrum of **1**. This material is available free of charge via the Internet at http://pubs.acs.org.

References and Notes

(1) Report of the global partners' meeting on neglected tropical diseases. World Health Organization 2007, http://whqlibdoc.who.int/hq/2007/WHO_CDS_NTD_2007.4_eng.pdf.
(2) Mayer, A. M.; Rodriguez, A. D.; Berlinck, R. G.; Hamann, M. T. *Comp. Biochem. Physiol. C: Pharmacol. Toxicol.* **2007**, *145*, 553–581.
(3) Mayer, A. M.; Rodriguez, A. D.; Berlinck, R. G.; Hamann, M. T. *Biochim. Biophys. Acta, Gen. Subj.* **2009**, *1790*, 283–308.
(4) Cachet, N.; Regalado, E. L.; Genta-Jouve, G.; Amade, P.; Thomas, O. P. *Steroids* **2009**, *74*, 746–750.
(5) Espada, A.; Jimenez, C.; Rodriguez, J.; Crews, P.; Riguera, R. *Tetrahedron* **1992**, *48*, 8685–8696, and references therein.
(6) Berlinck, R. G. S.; Burtoloso, A. C. B.; Kossuga, M. H. *Nat. Prod. Rep.* **2008**, *25*, 919–954.
(7) Schmitz, F. J.; Prasad, R. S.; Gopichand, Y.; Hossain, M. B.; Van der Helm, D.; Schmidt, P. *J. Am. Chem. Soc.* **1981**, *103*, 2467–2469.
(8) Holmes, C. F. B.; Luu, H. A.; Carrier, F.; Schmitz, F. J. *FEBS Lett.* **1990**, *270*, 216–218.
(9) Traore, F.; Faure, R.; Ollivier, E.; Gasquet, M.; Azas, N.; Debrauwer, L.; Keita, A.; Timon-David, P.; Balansard, G. *Planta Med.* **2000**, *66*, 368–371.
(10) Vaughan, A. M.; O'Neill, M. T.; Tarun, A. S.; Camargo, N.; Phuong, T. M.; Aly, A. S.; Cowman, A. F.; Kappe, S. H. *Cell. Microbiol.* **2009**, *11*, 506–520.
(11) Singh, A. P.; Surolia, N.; Surolia, A. *IUBMB Life* **2009**, *61*, 923–928.
(12) Agrawal, P. K. *Phytochemistry* **1992**, *31*, 3307–3330.
(13) König, W. A.; Benecke, I.; Bretting, H. *Angew. Chem., Int. Ed. Engl.* **1981**, *20*, 693–694.
(14) Cheng, S.-Y.; Dai, C.-F.; Duh, C.-Y. *Steroids* **2007**, *72*, 653–659.
(15) Huang, Y.-C.; Wen, Z.-H.; Wang, S.-K.; Hsu, C.-H.; Duh, C.-Y. *Steroids* **2008**, *73*, 1181–1186.
(16) Ma, K.; Li, W.; Fu, H.; Koike, K.; Lin, W.; van Ofwegen, L.; Fu, H. *Steroids* **2007**, *72*, 901–907.
(17) Burgoyne, D. L.; Andersen, R. J.; Allen, T. M. *J. Org. Chem.* **1992**, *57*, 525–528.
(18) Keyzers, R. A.; Northcote, P. T.; Webb, V. *J. Nat. Prod.* **2002**, *65*, 598–600.
(19) Plaza, A.; Perrone, A.; Balesrieri, M. L.; Felice, F.; Balestrieri, C.; Hamed, A. I.; Pizza, C.; Piacente, S. *Steroids* **2005**, *70*, 594–603.
(20) Gutierrez, M.; Capson, T. L.; Guzman, H. M.; Gonzalez, J.; Ortega-Barria, E.; Quinoa, E.; Riguera, R. *J. Nat. Prod.* **2006**, *69*, 1379–1383.
(21) Garzon, S. P.; Rodriguez, A. D.; Sanchez, J. A.; Ortega-Barria, E. *J. Nat. Prod.* **2005**, *68*, 1354–1359.
(22) Tasdemir, D.; Lack, G.; Brun, R.; Rüedi, P.; Scapozza, L.; Perozzo, R. *J. Med. Chem.* **2006**, *49*, 3345–3353.
(23) Baltz, T.; Baltz, D.; Giroud, C.; Crockett, J. *EMBO J.* **1985**, *4*, 1273–1277.
(24) Thuita, J. K.; Karanja, S. M.; Wenzler, T.; Mdachi, R. E.; Ngotho, J. M.; Kagira, J. M.; Tidwell, R.; Brun, R. *Acta Trop.* **2008**, *108*, 6–10.
(25) Räz, B.; Iten, M.; Grether-Bühler, Y.; Kaminsky, R.; Brun, R. *Acta Trop.* **1997**, *68*, 139–147.
(26) Buckner, F. S.; Verlinde, C. L.; La Flamme, A. C.; Van Voorhis, W. C. *Antimicrob. Agents Chemother.* **1996**, *40*, 2592–2597.
(27) Mikus, J.; Steverding, D. *Parasitol. Int.* **2000**, *48*, 265–269.

NP100348X